AN FDFD EIGENVALUE FORMULATION FOR COMPUTING PORT SOLUTIONS IN FDTD SIMULATORS

José A. Pereda, Ángel Vegas, Luis F. Velarde, and Oscar González
Departamento de Ingeniería de Comunicaciones (DICOM)
Universidad de Cantabria
Avda. Los Castros s/n
39005 Santander, Spain

Received 18 September 2004

ABSTRACT: *At the pre- and post-processing stages of a finite-difference time-domain (FDTD) simulation, important tasks are carried out that require knowledge of the port data (propagation constants, fields, impedances, and so on) of the problem structure. This paper introduces a 2D finite-difference frequency-domain (FDFD) eigenvalue formulation specifically tailored for the computation of port data to be used in conjunction with the 3D-FDTD method. A key feature of the proposed FDFD scheme is that it leads to the same numerical dispersion equation as that of the 3D-FDTD method. This means that, for a given frequency, the numerical propagation constants and mode patterns calculated by the two methods are identical. This is desirable for preserving the accuracy of the FDTD simulation.* © 2005 Wiley Periodicals, Inc.
Microwave Opt Technol Lett 45: 1–3, 2005; Published online in Wiley InterScience (www.interscience.wiley.com). DOI 10.1002/mop.20704

Key words: *finite-difference methods; numerical methods; electromagnetics*

1. INTRODUCTION

A number of external I/O ports are usually defined in the finite-difference time-domain (FDTD) simulation of microwave circuits. Each external port consists of a short section of uniform waveguide/transmission line terminated by suitable absorbing boundary conditions (ABCs). During an FDTD simulation, at the pre- and post-processing stages, important tasks are carried out which require knowledge of the port data (propagation constants, fields, impedances, and so on). Moreover, in order to perform some preprocessing tasks, such as the accurate tuning of one-way-wave ABCs and the setting up of sources to excite only the desired port modes, it is necessary to know the port data before starting the FDTD simulation. Post-processing tasks include the computation of scattering parameters and (possibly) their manipulation (for example, shifting the reference plane).

Several approaches have been reported for computing port data to be used in combination with FDTD simulations. For homogeneous rectangular waveguide ports, the propagation constants are usually calculated directly from the numerical dispersion equation and the mode patterns are analytically known [1]. For homogeneous arbitrarily shaped waveguides, cutoff frequencies and mode patterns have been obtained by using the finite-difference frequency-domain (FDFD) method [2]. For nonhomogeneous waveguiding structures, two main approaches have been reported. One consists of determining port data by using 2.5D-FDTD formulations [3, 4]. The other is based on computing the mode patterns [5] and propagation constants [6, 7] by means of the 3D-FDTD method.

The abovementioned time-domain techniques suffer from several drawbacks: the use of the 3D-FDTD method to determine port data is computationally demanding; 2.5D-FDTD techniques do not lead to true eigenvalue formulations, instead they result in a sort of transverse resonant problem [8]. This means that obtaining port data is difficult or even not feasible when complex modes in lossless ports are considered.

Dispersion diagrams and mode patterns are more naturally calculated by means of frequency-domain methods. The FDFD technique is thus a more appropriate choice. Moreover, this method leads to a true 2D eigenvalue problem.

When a differential problem is solved numerically by using a finite-difference (FD) scheme, the dispersion error inherent in each FD approximation leads to the waves in the resultant discrete domain being governed by a numerical-dispersion equation. As a result, not only are the numerical solutions different from the exact ones, but also different FD schemes lead to different numerical solutions.

At the pre- or post-processing stages of 3D-FDTD simulations, when we use port data obtained by another FD scheme, we are mixing numerical solutions governed by different numerical dispersion equations. This may result in a worsening of the overall accuracy. For example, "large errors are produced in the calculation of the multimode scattering parameters unless the proper evanescent constant is used" [9].

This paper introduces a 2D-FDFD eigenvalue formulation specifically tailored for the computation of port data to be used in conjunction with the 3D-FDTD method. A key feature of the proposed scheme is that it leads to the same numerical dispersion equation as the 3D-FDTD method. This means that, apart from round-off errors, for a given frequency the numerical propagation constants and mode patterns calculated by both methods are identical. This fact is illustrated by computing the dispersion diagram and the mode pattern of a dielectric-slab-loaded rectangular waveguide by means of the 3D-FDTD and the proposed 2D-FDFD methods.

2. THEORY

2.1. FDFD Eigenvalue Formulation

Consider the time-dependent Maxwell curl equations in dielectric media, given by

$$\nabla \times \vec{E} = -\mu_0 \frac{\partial \vec{H}}{\partial t}, \qquad \nabla \times \vec{H} = \varepsilon_0 \varepsilon_r \frac{\partial \vec{E}}{\partial t}.$$

By using Yee's scheme with spatial average for the calculation of the effective dielectric constants at dielectric interfaces, the above equations are approximated by the following difference expressions:

$$\mathbf{R}\vec{E}^n = -\mu_0 \frac{\boldsymbol{\delta}_t}{\Delta_t} \vec{H}^n \tag{1a}$$

$$\mathbf{R}\vec{H}^{n+(1/2)} = \varepsilon_0 [\bar{\varepsilon}_r] \frac{\boldsymbol{\delta}_t}{\Delta_t} \vec{E}^{n+(1/2)}, \tag{1b}$$

where

$$\mathbf{R} = \begin{pmatrix} 0 & -\dfrac{\delta_z}{\Delta_z} & \dfrac{\delta_y}{\Delta_y} \\ \dfrac{\delta_z}{\Delta_z} & 0 & -\dfrac{\delta_x}{\Delta_x} \\ -\dfrac{\delta_y}{\Delta_y} & \dfrac{\delta_x}{\Delta_x} & 0 \end{pmatrix}$$

represents the curl operator in discrete form and $[\bar{\varepsilon}_r] = \mathrm{diag}(\bar{\varepsilon}_{r_x}, \bar{\varepsilon}_{r_y}, \bar{\varepsilon}_{r_z})$ is the average dielectric constant. In the above expressions, $\boldsymbol{\delta}_\alpha$ ($\alpha = x, y, z, t$) is the centered finite-difference operator along the coordinate indicated by the subscript.

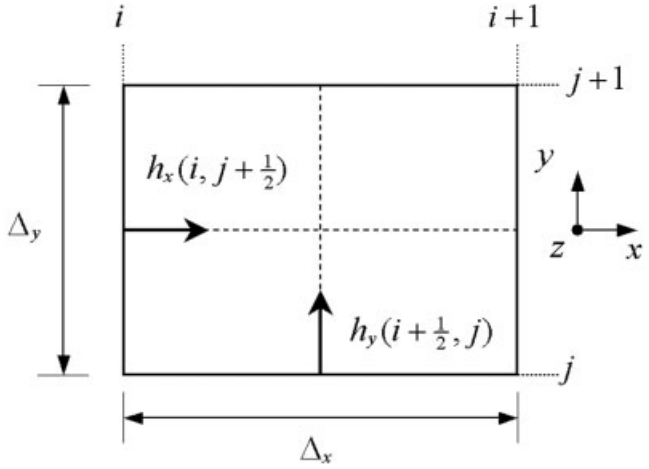

Figure 1 FDFD unit cell

Once Maxwell's equations have been discretized according to the 3D-FDTD method, the goal is now to derive a frequency-domain eigenvalue formulation for the computation of field patterns and propagation constants of the ports of the FDTD structure.

To this end, we consider solutions of the form

$$\vec{E}^n(i, j, k) = \{\vec{e}_t(i, j) + e_z(i, j)\,\hat{z}\}e^{\mathbf{j}\omega n\Delta_t - \tilde{\gamma}k\Delta_z},$$

$$\vec{H}^n(i, j, k) = \{\vec{h}_t(i, j) + h_z(i, j)\,\hat{z}\}e^{\mathbf{j}\omega n\Delta_t - \tilde{\gamma}k\Delta_z},$$

where $\tilde{\gamma}$ is the numerical propagation constant. The subscript t denotes quantities corresponding to coordinates perpendicular to the propagation direction. Substituting these expressions into Eqs. (1a) and (1b) and eliminating $\vec{e}_t$, e_z, and h_z, we arrive at the following FDFD equations:

$$\Gamma^2 h_x = -K_0^2\bar{\varepsilon}_{r_y}h_x - \frac{\boldsymbol{\delta}_x^2 h_x}{\Delta_x^2} - \frac{\boldsymbol{\delta}_x\boldsymbol{\delta}_y h_y}{\Delta_x\Delta_y} + \bar{\varepsilon}_{r_y}\frac{\boldsymbol{\delta}_y}{\Delta_y}\left\{\frac{1}{\bar{\varepsilon}_{r_z}}\left(\frac{\boldsymbol{\delta}_x h_y}{\Delta_x} - \frac{\boldsymbol{\delta}_y h_x}{\Delta_y}\right)\right\}, \tag{2a}$$

$$\Gamma^2 h_y = -K_0^2\bar{\varepsilon}_{r_x}h_y - \frac{\boldsymbol{\delta}_y^2 h_y}{\Delta_y^2} - \frac{\boldsymbol{\delta}_x\boldsymbol{\delta}_y h_x}{\Delta_x\Delta_y} - \bar{\varepsilon}_{r_x}\frac{\boldsymbol{\delta}_x}{\Delta_x}\left\{\frac{1}{\bar{\varepsilon}_{r_z}}\left(\frac{\boldsymbol{\delta}_x h_y}{\Delta_x} - \frac{\boldsymbol{\delta}_y h_x}{\Delta_y}\right)\right\}, \tag{2b}$$

where Γ and K_0 are given by

$$\Gamma = \frac{2}{\Delta_z}\sinh\left(\frac{\tilde{\gamma}\Delta_z}{2}\right), \qquad K_0 = \frac{2}{c\Delta_t}\sin\left(\frac{\omega\Delta_t}{2}\right).$$

The port cross-section is discretized by using the unit cell shown in Figure 1. This cell is obtained by simply collapsing the 3D Yee cell in the z direction and eliminating from it the field components not directly involved in the formulation. Eq. (2a) is evaluated at nodes $(i, j + 1/2)$ and Eq. (2b) at nodes $(i + 1/2, j)$.

Transforming the double index scheme used in the above development, (i, j), into a single index scheme and applying Eqs. (2a) and (2b) to the whole port cross-section, we arrive at the following eigenvalue problem:

$$[A][h_t] = \{\Gamma^2[I] + K_0^2[\bar{\varepsilon}_{rt}]\}[h_t], \tag{3}$$

where $[A]$ is a sparse data matrix, $[I]$ is the identity matrix, $[\bar{\varepsilon}_{rt}]$ is a diagonal matrix, and $[h_t] = [h_x(1), \ldots, h_x(n_x), h_y(1), \ldots, h_y(n_y)]^T$, with n_x and n_y being the number of h_x and h_y unknowns, respectively. Eq. (3) can be used in two alternative ways: (i) considering that the frequency is known and solving the resulting eigenvalue problem,

$$\{[A] - K_0^2[\bar{\varepsilon}_{rt}]\}[h_t] = \Gamma^2[h_t],$$

for the numerical propagation constant; or (ii) assuming that $\tilde{\gamma}$ is known and solving

$$[\bar{\varepsilon}_{rt}]^{-1}\{[A] - \Gamma^2[I]\}[h_t] = K_0^2[h_t]$$

for the frequency. The latter choice can be used, for instance, to compute numerical cutoff frequencies by simply letting $\tilde{\gamma} = 0$.

2.2. Numerical Dispersion Equation

Analogously to the FDTD case, in order to obtain the numerical dispersion equation for the above FDFD formulation, we consider homogeneous media and we substitute into Eq. (2) solutions of the form:

$$h_\alpha(i, j) = h_{\alpha 0}e^{-\mathbf{j}\tilde{k}_x i\Delta_x}e^{-\mathbf{j}\tilde{k}_y j\Delta_y}, \quad (\alpha = x, y),$$

which leads to the following dispersion equation:

$$\frac{\varepsilon_r}{c^2\Delta_t^2}\sin^2\left(\frac{\omega\Delta_t}{2}\right) = \frac{1}{\Delta_x^2}\sin^2\left(\frac{\tilde{k}_x\Delta_x}{2}\right) + \frac{1}{\Delta_y^2}\sin^2\left(\frac{\tilde{k}_y\Delta_y}{2}\right) - \frac{1}{\Delta_z^2}\sinh^2\left(\frac{\tilde{\gamma}\Delta_z}{2}\right). \tag{4}$$

It can be seen that Eq. (4) has the same form as the 3D-FDTD numerical dispersion equation (see, for instance, [9]).

3. NUMERICAL VALIDATION

To illustrate port-data computation by the proposed FDFD formulation, we have considered a rectangular waveguide loaded with a dielectric slab. The dimensions of the waveguide are $a \times a/2$ with $a = 19.05$ mm (WR75). The dimensions of the dielectric slab are $2a/5 \times a/2$, its dielectric constant is $\varepsilon_r = 4$, and it is in contact

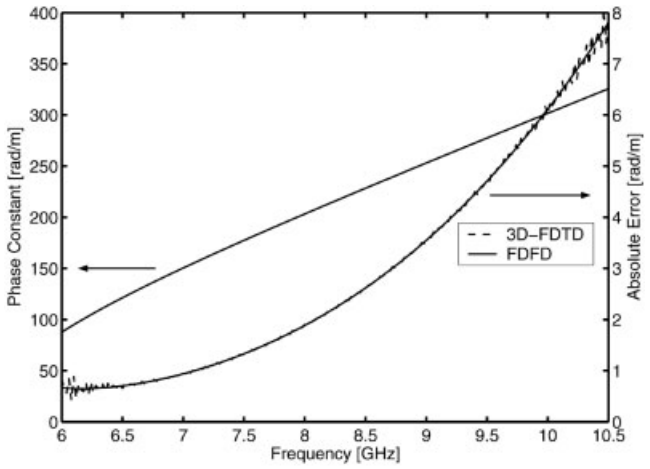

Figure 2 Left axis: exact phase constant; right axis: phase constant absolute error obtained by the 3D-FDTD (dashed line) and by the FDFD (solid line) methods

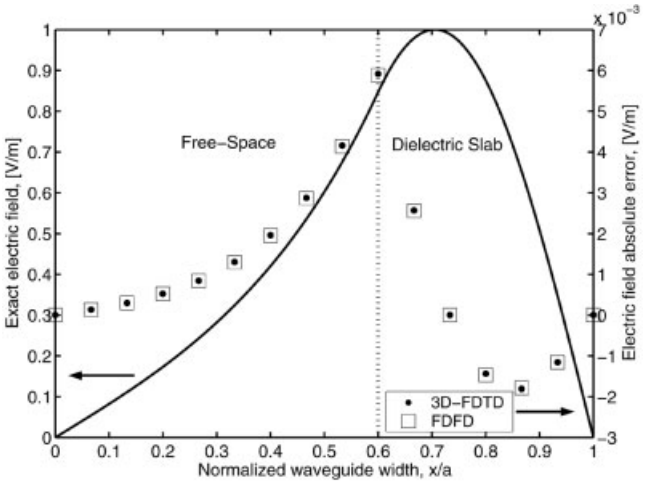

Figure 3 Left axis: exact E_y; right axis: absolute error for E_y obtained by the 3D-FDTD (dots) and by the FDFD (squares) methods

with a narrow wall of the waveguide. The exact solution of this structure can be obtained by solving its characteristic equation [10].

Figure 2 shows the exact data for the phase constant of the TE_{10} mode (left axis), and the absolute error of the phase constant for the same mode when the calculation is made by using the 3D-FDTD method (right axis, dashed line) and by the FDFD method (right axis, solid line). These results have been obtained for a frequency band that runs from 6 to 10.5 GHz. It can be seen that the two error curves coincide at the central part of the band, while a small ripple is observed for the 3D-FDTD data at both ends of the band. This ripple is a consequence of the truncation of the time-domain response. When obtaining these results, we used the same discretization in the transverse plane (15×5) and identical values of Δ_z and Δ_t for both methods.

Figure 3 depicts the exact E_y field, at 9 GHz, for the mode TE_{10} (left axis) and the corresponding absolute error when E_y is computed by the 3D-FDTD method (right axis, dots) and by the FDFD method (right axis, squares). It can be seen that both FD techniques lead to the same numerical results.

4. CONCLUSION

This paper has introduced a 2D-FDFD eigenvalue formulation specifically tailored for the computation of port data to be used in combination with the 3D-FDTD method. The proposed FDFD scheme leads to the same numerical dispersion equation as the 3D-FDTD method. Port data obtained by the proposed FDFD formulation can be used not only at the pre- and post-processing stages of a 3D-FDTD simulation, but also to study the impact of the FDTD discretization process on magnitudes of interest such as propagation constants, fields, cutoff frequencies, impedances, and so forth.

ACKNOWLEDGMENT

This work was supported by the Spanish Dirección General de Investigación under project no. TIC2003-09677-C03-01.

REFERENCES

1. L.A. Vielva, J.A. Pereda, A. Vegas, and A. Prieto, Multimode characterization of waveguide devices using absorbing boundary conditions for propagating and evanescent modes, IEEE Microwave Guided Wave Lett 4 (1994), 160–162.
2. M. Werten, M. Rittweger, and I. Wolff, Multi-mode simulation of homogeneous waveguide components using a combination of FDTD and FD^2 method, Proc 25th EuMC, Bologna, Italy, 1995, pp. 234–237.
3. A. Asi and L. Shafai, Dispersion analysis of anisotropic inhomogeneous waveguides using compact 2D-FDTD, Electron Lett 28 (1992), 1451–1452; Corrections, Electron Lett 29 (1993), 423.
4. S. Xiao, R. Vahldieck, and H. Jin, Full-wave analysis of guided wave structures using a novel 2-D FDTD, IEEE Microwave Guided Wave Lett 2 (1992), 165–167.
5. C.J. Railton and J.P. McGeehan, The use of mode templates to improve the accuracy of the finite-difference time-domain method, Proc 21st EuMC, Stuttgart, Germany, 1991, pp. 1278–1283.
6. W.K. Gwarek and M. Celuch-Marcysiak, A differential method of reflection coefficient extraction from FDTD simulations, IEEE Microwave Guided Wave Lett 6 (1996), 215–217.
7. M.A. Schamberger, S. Kosanovich, and R. Mittra, Parameter extraction and correction for transmission lines and discontinuities using the finite-difference time-domain method, IEEE Trans Microwave Theory Tech 44 (1996), 919–925.
8. J.A. Pereda, J.E. Fernández del Río, F. Wysocka-Schillak, A. Prieto, and A. Vegas, On the use of linear prediction techniques to improve the computational efficiency of the FDTD method for the analysis of resonant structures, IEEE Trans Microwave Theory Tech 46 (1998), 1027–1032.
9. E.A. Navarro, T.M. Bordallo, and J. Navasquillo-Miralles, FDTD characterization of evanescent modes: Multimode analysis of waveguide discontinuities, IEEE Trans Microwave Theory Tech 48 (2000), 606–610.
10. R.E. Collin, Field theory of guided waves, 2nd ed., IEEE Press, New York, 1991.

© 2005 Wiley Periodicals, Inc.

DUAL-FREQUENCY MICROSTRIP ANTENNAS

Feng-Pin Chuo, Tsair-Rong Chen, and Jeen-Sheen Row
Department of Electrical Engineering
National Changhua University of Education
Chang-Hua, Taiwan 500, R.O.C.

Received 25 September 2004

ABSTRACT: *This paper presents the design of a dual-port microstrip patch antenna with dual-frequency operation. Two different feed mechanisms—aperture coupling and inset coplanar microstrip line—are used to excite the TM_{10} and TM_{01} modes, respectively, on a single square patch. The frequency ratio of the proposed dual-frequency microstrip antenna can be varied by changing the inset length of the coplanar microstrip line while the peripheral dimensions of the patch are fixed. Several prototype antennas operating at frequency ratios ranging from 1.04 to 1.36 are constructed and tested. The experimental results show that the isolation level between the two input ports of the proposed dual-frequency antenna is primarily determined by its operating-frequency ratio.*
© 2005 Wiley Periodicals, Inc. Microwave Opt Technol Lett 45: 3–5, 2005; Published online in Wiley InterScience (www.interscience.wiley.com). DOI 10.1002/mop.20705

Key words: *dual-frequency; dual-polarization; microstrip antenna*

1. INTRODUCTION

With the increase of multichannel wireless communications, a compact antenna having dual-frequency and dual-polarization operation is required at base stations. Microstrip patch antennas are considered promising candidates due to their low profile and easy integration with front-end circuits. In addition, two orthogonal